Mechanisms and models of the dehydration self-organization in biological fluids

2004 Phys.-Usp. 47 717

(http://iopscience.iop.org/1063-7869/47/7/R05)

Physics – Uspekhi **47** (7) 717 – 728 (2004)

FROM THE CURRENT LITERATURE PACS numbers: 68.03.Fg, **82.70. – y**, 87.19.Tt

Mechanisms and models of the dehydration self-organization in biological fluids

Yu Yu Tarasevich

DOI: 10.1070/PU2004v047n07ABEH001758

Contents

Abstract. The dehydration self-organization phenomenon in biological fluids attracted the attention of researchers slightly more than a decade ago. While seemingly simple (the structure formation is possible to observe even in domestic conditions), the effect turned out to be extremely complicated and to involve a number of interrelated processes of a different physical nature. The dehydration self-organization effect in biological fluids underlies a medical diagnostic technique patented in 40 countries of the world, while the mechanisms that underlie the technique still remain largely obscure. This review is an attempt to draw an integrated picture of the current state of the problem: to emphasize reliably established facts and the problems that remain to be solved, to put an end to speculation, and to characterize the available theories and models. An analysis of the literature sources allows us to draw the conclusion that the effects observed in the dehydration of biological fluids are typical for colloidal solutions in general and can be described in the framework of conventional physical approaches.

Yu Yu Tarasevich Astrakhan' State University,
Institute for Physics and Mathematics
ul. Tatishcheva 20a, 414056 Astrakhan', Russian Federation
Tel. (7-8512) 549 097. Fax (7-8512) 251 718
E-mail: tarasevich@astranet.ru

Received 11 October 2003, revised 22 December 2003
Uspekhi Fizicheskikh Nauk **174** (7) 779 – 790 (2004)
Translated by E N Ragozin; edited by A Radzig

"*Nature is simple and does not luxuriate with excessive causes of things*".
Isaac Newton *Philosophiae Naturalis Principia Mathematica*

1. Introduction

The effect of dehydration self-organization of biological fluids attracted the attention of researchers slightly more than a decade ago. On the one hand, it is stated that the priority in the investigation of the effect belongs to E G Rapis (the work has been pursued since 1976; see Ref. [1]). On the other hand, V N Shabalin and S N Shatokhina argue that they have been exploring the effect since 1986 [2].

At present, publications on the dehydration self-organization of biological fluids are uncoordinated in character and belong primarily to the medical profession. The series of papers by Rapis is concerned with the phenomenological description of separate processes discovered in the dehydration self-organization, for instance, the variation of magnetic sensitivity of protein. The works of Shabalin and Shatokhina are concerned primarily with the description of structures revealed in the course of one pathological process or another. Our attention is drawn to the fact that the papers of Shabalin and Shatokhina contain no references to the papers by Rapis, and vice versa. Their descriptions of the structures do not always prove to be easily understood: "In the final solid phase we discovered the formation of a polyfilm solid material, three-dimensional spatial dissipative nanostructures with nucleation, fractal geometry with autocatalysis and self-complementary properties" [3, p. 104]. The available papers by different groups of authors dedicated to the investigation of structure formation in the drying of a colloidal solution droplet heretofore have not been associated to similar processes in biological fluids.

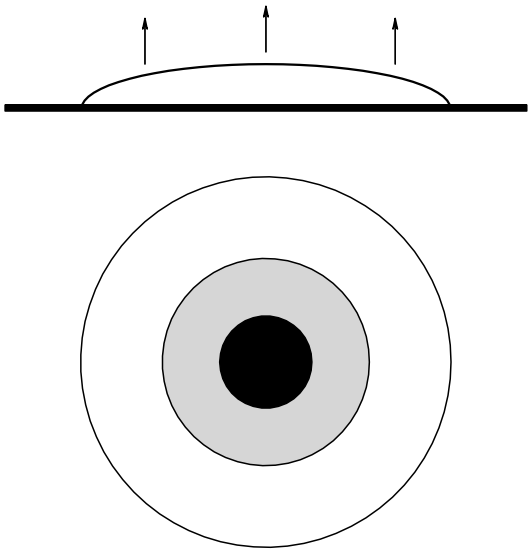

Figure 1. Schematic drawings of a droplet of biological fluid on a plane: the upper drawing shows the side elevation, and the lower one the top view. Shown in white is the region which primarily accumulates proteins when the droplet dries, in black the region which primarily accumulates salt, and in gray the transition region (taken from Ref. [2]).

To observe the phenomenon of interest, advantage is commonly taken of a method referred to as the *wedge-shaped dehydration technique* [4]: a droplet of a biological fluid (blood serum, saliva, histological or spinal fluid, etc.) is deposited on a strictly horizontal degreased microscope slide with a dispensing apparatus. The droplet volume ranges 10 – 20 μl. The diameter of the droplet on the microscope slide is 5 – 7 mm. The average thickness is about 1 mm. The slope of the droplet surface measures 25 – 30° [4]. The sample is dried out at a temperature of 20 – 25 °C and a relative humidity of 65 – 70%. The drying lasts for 18 – 24 h. The dried droplet of the biological fluid is termed a *film* [1] or a *facies*[1] [4] and is structurally complex (Figs 1 and 2). In accordance with the data of Refs [5, 6], the central region should be termed the *region of crystalline structures*, and the peripheral one the *amorphous region*. The transition region shows up only when blood serum is used for the biological fluid, while the transition region is hardly present when use is made of other biological fluids (for instance, of spinal fluid). The ratio between the width of the protein region and the diameter of the entire sample is employed for determining the content of proteins in the biological fluid [2, pp. 239 – 241]. The visual appearance of a facies is used for diagnosing a wide range of diseases [2]. In particular, radial regular cracking of a sample of blood serum is typical for a healthy person, while for a sick person there is chaotic cracking (see Fig. 2[2]). The authors of the above technique actively promote and publicize it, suggesting the following law as its scientific substantiation: "All kinds of interaction between material objects constitute counterpropagating autowave flows in an electromagnetic field, which are produced by the self-oscillatory motion of these objects" [2, p. 45].

At the present time, investigations of the problem are in the stage of phenomenological description. A wealth of experimental material has been accumulated (8,000 samples were investigated by Rapis alone, and more than 10,000 by Shabalin and Shatokhina). It has been established that the structural formation of a biological fluid dehydrating in an open volume on a solid substrate has clear regularities (the phenomenon of dehydration self-organization). Rather clear relationships of the 'form of observed structures — pathological process' type have been revealed. Presented in the literature are the data on the visual appearance variation of the film of a dried droplet of blood serum for patients with carcinoma, viral hepatitis type B, Waldenstrom's disease, paraproteinemic hemoblastosis, burn disease, tuberculosis, and leprosy, as well as for women who have had normal and premature deliveries [2, 8, 9].

Despite the application of the method to practical medical diagnostics, the theoretical description of the dehydration self-organization in biological fluids is lacking. Efforts mounted by Shabalin and Shatokhina to provide a theoretical substantiation for the method can hardly be accepted as satisfactory: "In conformity with the data of modern physics it is valid to say that the autowaves of biological structures are formed by the autowaves of their elements, whose rhythms undergo, due to cooperative interaction, gauge synchronization and determine the autowave characteristics of the integral object" [2, p. 36].

The biophysical, biochemical, and biological processes occurring in the dehydration of biological fluids remain largely to be clarified.

At the same time, an analysis of the literature sources can lead to the conclusion that the phenomena observed in the dehydration of biological fluids are characteristic of colloidal solutions altogether, that individual processes and effects have been adequately studied, and that efficient models have been suggested for their description.

Our review is an attempt to collect together the separate information and present an integrated picture of the current state of the problem.

2. Processes observed in the dehydration of biological fluids

In this section we present the generalized data from Refs [2, 4, 10, 11].

The following processes are observed in the dehydration of biological fluids.

(1) Directional motion of the particles of substances. Shabalin and Shatokhina [2] point to the radial outward motion of the particles. This motion is typical of drying droplets of solutions, including colloidal ones, and was studied at length in Refs [12 – 14]. The main findings of these investigations will be outlined in Section 4. Furthermore, the occurrence of rotation of the entire mass of water in the droplet in the form of a torus is indicated, and in rare instances associated with a serious pathology the counterclockwise rotation of the entire mass of solution is also observed. Such rotation is supposedly related to the development of Marangoni instability (see Section 5).

(2) The droplet drying begins at the periphery. The formation of concentric annular structures is observed in the process. Golbraikh et al. [10] attribute the emergence of these

[1] Facies are the strata or suites of strata of sedimentary rocks characterized by a specific composition and the same organic residues (for instance, sand, lime, or coral facies [7]. Wide use of terminology borrowed from other subject areas is typical for the papers written by Shabalin and Shatokhina. In many instances, the terminology employed is controversial.

[2] A K Ayupova from the Leprosy Research Institute kindly provided us with figures 2 and 3.

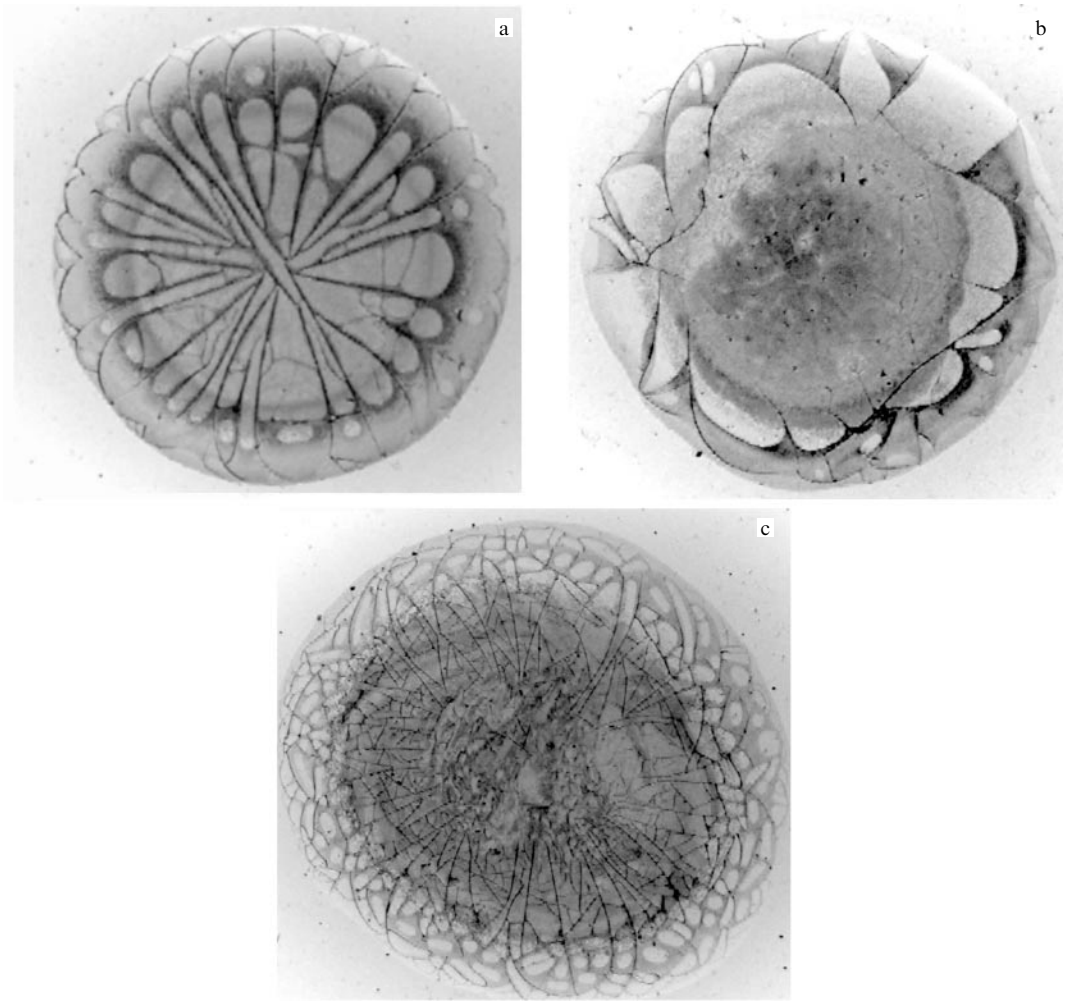

Figure 2. (a) Sample of the dried droplet of blood serum of a practically healthy person. (b, c) Samples of the dried droplets of blood serum of people with chronic diseases.

structures to either the stagnation points or standing concentration autowaves. Similar structures were observed in dilute colloidal solutions of an inorganic nature [14]. As noted in Ref. [2], the motion of the solid phase boundary to the center takes place in 10 – 20 μm jumps 1 – 2 s apart.

(3) The ring-shaped dried protein film produced at the periphery begins to crack towards the center. When employing the blood serum of a healthy person as the sample, the cracking is regular: the cracks are separated by nearly equal distances and form a 'camomile' (Fig. 2a). When employing the blood serum of a sick person as the sample, the cracking is chaotic in character. Pauchard et al. [15] carried out a comprehensive investigation into the effect of ionic strength [3] of a solution on the character of the crack pattern produced in the drying of a droplet of the colloidal solution. They showed that the crack pattern is determined by the ratio between the droplet drying time and the gelation time. The main results will be outlined in Section 6.

(4) Formation of a cellular structure in the sectors. Upon further film drying, the sectors begin to crack and in the process form a cellular structure, according to the terminology of Refs [3, 10], or the *separates*, to follow the terminology of Ref. [2].

(5) *Nuclei* or *concretions* [4] begin to form in the sectors [2]. The statement that these nuclei are made up of salts [2, 4] are not borne out by experiments. Spiral cracks may form around the nuclei. The model of spiral crack production was put forward in Ref. [10] and is briefly outlined in Section 8.

(6) When studying the samples of blood serum from sick people it was possible to observe additional structures in the form of plaques, wrinkles, Sierpinski's carpets, and Arnold's tongues [5] [2, 4] (Fig. 3). In blood serum samples obtained from patients, Yakhno et al. [9] observed crystalline structures resembling immunoglobulin M (IgM) in shape, which exceeded it by a factor of 1000.

(7) Crystalline structures may form in the central part of a sample.

(8) When the sample is an aqueous solution of a protein, in several days, weeks, and months in the surface layer of the

[3] The ionic strength of a solution is defined as $I = (1/2)\sum_i C_i Z_i^2$, where C_i is the ith ion concentration, and Z_i is its valency.

[4] "*Concretions* [Latin *concretio* — thickening] — variously shaped (most often more or less rounded) mineral structures in sedimentary rocks which constitute accumulations of similar or different minerals that differ from the surrounding rock; they are formed owing to the contraction of materials scattered in the rock and their accumulation around some centers" [7].

[5] *Arnold's tongues* — regions of synchronization of circle mapping (see, for instance, Ref. [16]). This term is supposedly employed because the observed structures bear a superficial resemblance to synchronization regions.

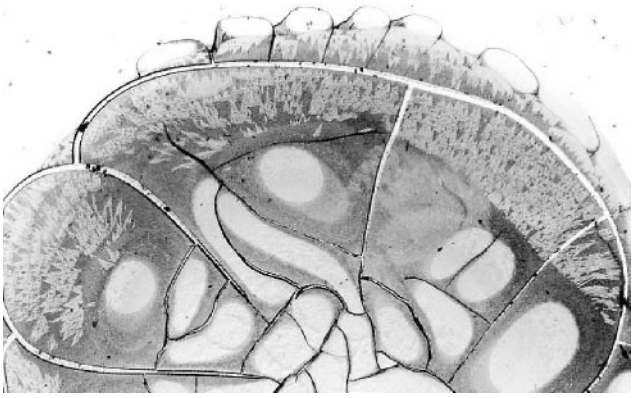

Figure 3. Arnold's tongues in a human blood serum sample.

sample there form filamentary structures referred to as *filaments*[6] in Ref. [11].

Therefore, diversified processes occur and different structures are produced in the drying of a droplet of a biological fluid. The results of a more thorough investigation into the mechanisms of individual processes and the models proposed for their description are outlined in the sections that follow.

3. Precipitation near the perimeter of a drying droplet

A characteristic feature of the drying of a droplet of a colloidal solution or a solution with admixtures on a solid surface is the *pinning* (adhesion) of the interphase boundary: in the course of drying, the area of droplet contact with the solid substrate does not change and the interface remains immobile. The forces that confine the interphase boundary may arise due to roughnesses of the surface or its chemical inhomogeneity. Unlike the evaporation of a pure water droplet on a smooth substrate, when the contact angle remains invariable, a suspension droplet evaporates at a constant area of the contact with the surface. Early in the evaporation process, the suspension particles settle to the substrate and impede the interface motion. As a result, the contact angle changes during evaporation, and the droplet shape experiences strong distortions.

Deegan [14] introduced the notion of *self-pinning* — that is, the pinning caused by the properties of the liquid droplet itself rather than the properties of the substrate. To eliminate the pinning arising from irregularities in the solid substrate, advantage was taken of a mica plate freshly cleaved with the aid of a special-purpose technique, which ensured a surface roughness on the order of atomic dimensions. When a pure water droplet was deposited on the mica surface, it decreased in diameter in the course of evaporation. In the case of a colloidal solution of polystyrene (with a volume fraction of polystyrene equal to only 2%), the droplet diameter remained invariable on drying.

For an ordinary surface, the interphase boundary may temporarily adhere to random surface irregularities, which is the starting point for the precipitation in droplet evaporation. The precipitated particles produce an additional energy barrier impeding the displacement of the interphase boundary, and the latter becomes immobile once and for all.

The precipitation effect near the perimeter of the drying droplet was extensively investigated in Refs [12–14]. Based on a large number of experiments with different substances, solvents, and substrates, a conclusion was reached that the effect is invariable over a wide range of experimental conditions. The annular precipitate was observed with the use of different substrates: glass, metal, rough teflon, freshly cleaved mica, ceramics, and silicone. The rings were detected both in large drops (15 cm) and small droplets (1 mm). Water, acetone, methanol, toluene, and ethanol were utilized as solvents. The annular precipitate was observed for molecular-sized solutions (sugar and dyes) and colloidal solutions (polystyrene microspheres in sizes up to 10 μm). The volume fraction of the dissolved substance in the solvent ranged from 10^{-6} to 10^{-1}.

It was shown that the phenomenon of interest was scarcely affected by diffusion effects, gravitation, electrostatic fields, or surface tension. When using colloidal solutions with microparticles ranging from 1 to 10 μm in size, it was possible to observe the unidirectional radial particle motion away from the droplet center. A local heating of the droplet gave rise to circular fluid motion in it, but the precipitation in the form of a ring persisted.

A conclusion was drawn that the annular precipitation was determined by two effects: the effect of pinning of the droplet edge, and evaporation. When smooth teflon was used as the substrate, the droplet diameter decreased during evaporation and the precipitation proceeded uniformly and not in the form of a ring. A more uniform precipitation was also detected when droplet evaporation was limited. To limit evaporation, the droplet was covered with a lid with a small central opening. The lid kept the droplet from evaporating at the edge.

Underlying the theory by Deegan et al. [13] of annular precipitation in droplet evaporation is the idea that pinning is accompanied by a radial fluid flow towards the droplet edge (Fig. 4).

From the fluid mass conservation law it follows that

$$\rho\,\frac{\partial h}{\partial t} = -\rho\,\frac{1}{r}\,\frac{\partial}{\partial r}(rhv) - J_s(r,t)\sqrt{1+\left(\frac{\partial h}{\partial r}\right)^2}\,, \qquad (1)$$

where t is the time, ρ is the fluid density, v is the height-averaged radial velocity of the fluid flow, h is the location of

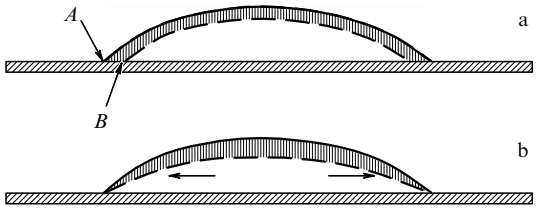

Figure 4. Schematic drawing explaining the cause for the emergence of horizontal flow. (a) If the interphase boundary line is mobile, a uniform evaporation is responsible for the displacement of the droplet–air boundary from the position shown with the solid line to the position shown with a dashed line. The hatched layer of the droplet evaporates. The interphase boundary shifts from point A to point B. (b) Actual displacement of the droplet surface for an immobile interphase boundary line. The displacement of the latter line from point A to point B is impeded by the horizontal flow directed from the center of the droplet towards its edges.

[6] The term *filaments* in biology is commonly used in reference to filamentary protein structures.

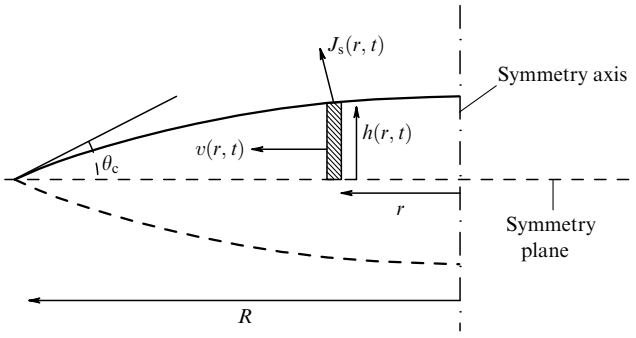

Figure 5. Schematic diagram illustrating the fluid mass conservation law [formula (1)].

the fluid–air boundary, and J_s is the mass of water evaporating per unit droplet surface area per unit time (Fig. 5). The term $\partial h/\partial r$ is negligible almost without exception.

The flow velocity can be expressed from Eqn (1) by rewriting it in the integral form

$$v(r,t) = -\frac{1}{\rho r h}\int_0^r r\left(J_s(r,t)\sqrt{1+\left(\frac{\partial h}{\partial r}\right)^2}+\rho\,\frac{\partial h}{\partial t}\right)\mathrm{d}r\,. \quad (2)$$

To calculate v requires determining h and J_s. The droplet profile $h(r,t)$ is defined by the Navier–Stokes equation; however, it may be suggested that the droplet is a spherical segment. Physically, this assumption corresponds to a droplet of small radius, when the surface tension forces tending to impart a spherical shape to the droplet are much stronger than the gravitational forces which seek to flatten the droplet (the Bond number is much smaller than unity:

$$\mathrm{Bo} = \frac{g(\rho-\rho_f)d^2}{\sigma} \ll 1\,,$$

where g is the free fall acceleration, ρ is the density of the droplet substance, ρ_f is the density of the medium in which the droplet is located, σ is the surface tension coefficient, and d is the droplet diameter).

Experiments performed to measure the droplet profile during evaporation confirmed that the droplet has the shape of a spherical segment. Furthermore, the evaporation should proceed slow enough for the dynamic contribution to the pressure, as well as the viscosity-related energy dissipation, to be disregarded. Therefore, we consider the hydrostatic limit and only the $\nabla p = 0$ term is retained in the Navier–Stokes equation:

$$h(r,t) = \sqrt{\left(\frac{h(0,t)^2+R^2}{2h(0,t)}\right)^2 - r^2} - \frac{R^2-h(0,t)^2}{2h(0,t)}\,, \quad (3)$$

where $h(0,t)$ is the droplet height at the center.

The form of the J_s function is determined by the character of evaporation process. Two regimes are distinguished. In the first case, the evaporation rate is determined by the rate of mass transfer across the liquid–gas interface (the flux J_s is constant in that event), and in the second case by the diffusional relaxation of the saturated vapor layer above the droplet (in that instance, J_s increases towards the droplet edges).

When the vapor diffusion is the limiting factor, it is assumed that the droplet evaporation rapidly attains the stationary state, i.e., the diffusion equation goes over to the Laplace equation

$$\frac{\partial u}{\partial t} = D\Delta u \approx 0\,, \quad (4)$$

where u is the vapor mass per unit volume of the air, and D is the vapor diffusion coefficient in the air. This assumption is valid for times exceeding D/R^2 (i.e., for a water droplet of 1 mm radius this quantity is equal to 0.04 s).

The boundary conditions are as follows:

(i) the vapor at the droplet surface is saturated ($u = u_s$);

(ii) the flow directed perpendicular to the substrate surface is zero because the substrate is impenetrable by the vapor;

(iii) away from the droplet, the density u tends to the value u_∞.

The problem under consideration is equivalent to the problem of a charged conductor if u is treated as the electrostatic potential, and J as the intensity of the electric field.

Near the interphase boundary, one finds

$$J_s(r,t) \sim (R-r)^{-\lambda}\,, \quad (5)$$

where $\lambda = (\pi - 2\theta_c)/(2\pi - 2\theta_c)$, and θ_c is the contact angle.

With the knowledge of $J_s(r,t)$ it is possible to derive the dependence $h(0,t)$. The droplet mass variation should be precisely equal to the evaporation rate:

$$\frac{\mathrm{d}M}{\mathrm{d}t} = \rho\,\frac{\mathrm{d}}{\mathrm{d}t}\int_0^R 2\pi r' h(r',t)\,\mathrm{d}r' = \int_0^R 2\pi r' J_s(r',t)\sqrt{1+\left(\frac{\partial}{\partial r'}\,h(r',t)\right)^2}\,\mathrm{d}r'\,. \quad (6)$$

$J_s(r,t)$ exhibits a nontrivial time dependence because this quantity depends on the contact angle which changes in the course of droplet evaporation.

Having determined the flow velocity inside the droplet it is possible to calculate the mass of the annular precipitate:

$$m_R\big(t(r_0)\big) = 2\pi c_0\int_{r_0}^R r' h(r',t=0)\,\mathrm{d}r'\,, \quad (7)$$

where c_0 is the solution concentration, and $t(r_0)$ is the time required for the displacement from $r = r_0$ at $t = 0$ to $r = R$. This quantity can be determined by integrating $\mathrm{d}r/\mathrm{d}t = v(r)$ subject to the initial condition $r(0) = r_0$. Since use is made of the height-averaged velocity, the vertical separation of the solution is assumed to be lacking. Then, the conservation law for the solution acquires the form

$$\frac{\partial}{\partial t}(ch) + \frac{1}{r}\,\frac{\partial}{\partial r}(rchv) = 0\,, \quad (8)$$

where c is assumed to be z-independent, and the diffusion effects are disregarded. Furthermore, the ring mass can be defined as the difference between the initial droplet mass and the solution mass at a given point in time.

In the context of this theory, several important qualitative results have been obtained analytically.

Deegan et al. [13] indicated the factors which may turn out to be significant in a number of cases.

(i) Nonuniform solute distribution along the height of the droplet. For large-sized particles, the sedimentation effect

may turn out to be significant. For a solution containing a mixture of substances with particles of different sizes, stratification of the solution is quite possible.

(ii) Viscosity effects may lead to distortions in the droplet shape, especially near the edge, where the horizontal flow velocity diverges and the corresponding term in the Navier–Stokes equation may become dominant. For viscous fluids, among which are, for instance, biological fluids, the droplet shape distortions can extend over a considerable distance from the edge.

(iii) For concentrated solutions, the dependence of the solution viscosity on the concentration may prove to be of significance.

(iv) In the case of particles with a small radius, diffusion effects may prove to be comparable to the horizontal flow effect.

The last-listed remark is of special interest, because real biological fluids comprise both large molecules (proteins) and small ones (salts).

It is pertinent to note that there exists a different interpretation for the cause of the occurrence of the horizontal flow in the droplet. This interpretation comes from to Shabalin and Shatokhina: "Since the power of osmotic forces is two orders of magnitude higher than that of oncotic ones, salts and permolecular complexes with a large content of salts begin to move towards the droplet center — that is, towards the lower density of dissolved substances. The molecules and permolecular structures with a low osmotic activity move in the opposite direction, namely, to the droplet edge. In the struggle for the remaining water the salts 'press back' the organic substances to the peripheral region of the droplet. The difference in osmotic activity is so large that the salts thicken the organic components of the biological fluid to form a rise in the form of a bolster at the periphery of the drying droplet"[7] [4, p. 46]. We believe that the hypothesis involving the struggle of osmotic and oncotic forces is superfluous; the phenomenon can well be explained in the context of the approach outlined in this section. Besides, additional information on the profile formation for the drying droplet of a colloidal solution can be drawn in Section 6.

4. Effect of diffusion processes

Tarasevich and Ayupova [17] theoretically investigated diffusion processes and showed that they favor a more uniform salt distribution along the droplet radius and have little or no effect on the protein concentration distribution. The initial stage of droplet evaporation was considered in the paper, when the vapor flux from the droplet surface can be treated as uniform. In this case, the evaporation is determined by the rate of mass transfer across the liquid–vapor interface rather than the vapor diffusion rate, as in the case of a stationary evaporation regime. Furthermore, recourse is made to a simplified geometry of the problem: the droplet surface is assumed to be flat and inclined. The equation for the upper wedge side is written in the form

$$y = h_0 - kr - vt\,;$$

here, h_0 is the maximum droplet thickness, α is the slope angle ($\tan\alpha = k$), and v is the velocity of free-surface displacement arising from evaporation.

The albumin and salt diffusion coefficients are assumed to be independent of the substance concentrations.

In the context of this approach, the spatial variation of the concentration of dissolved substances is determined by the evaporation of the solvent as well as by diffusion. The relative significance of these effects can be estimated with the aid of the dimensionless coefficient

$$d = k^2\,\frac{D}{h_0^2}\,\frac{h_0}{v} = k^2\,\frac{\tau_{\text{shift}}}{\tau_{\text{diff}}}\,.$$

Here, D is the diffusion coefficient, τ_{shift} is the characteristic shift time of the upper wedge side, and τ_{diff} is the relaxation time (the time it takes the substance concentration to change by a factor of e due to diffusion). Therefore, the coefficient d determines which of the processes — those of diffusion or concentration variation due to evaporation — prevail in this case.

An estimate of the parameter d gives a value on the order of 0.01 for proteins, and a unity for salt. Therefore, the protein concentration dynamics is scarcely affected by diffusion.

Calculations confirm the above estimate signifying that diffusion does not play a decisive role in the variation of protein concentration in the course of wedge dehydration. At the same time, the diffusion smooths to a large measure the effect of salt density growth towards the droplet edge.

The proposed model allows us to explain the spatial redistribution of the components of biological fluids in the course of wedge dehydration. In the absence of diffusion, the relative concentration of salt and protein at various points in space would remain constant, the absolute concentration of the substances increasing towards the droplet edge. The theoretical possibility of including the effects of cross-diffusion and concentration dependence of diffusion coefficients was not realized owing to a lack of experimental data. However, the effects unaccounted for can be estimated at a qualitative level. A decrease in the diffusion coefficient of protein with an increase in its concentration would moderate the effect of diffusion concentration equalization. The spatial protein concentration distribution would be still closer to that which results from inclusion of only the fluid evaporation. An increase in the salt diffusion coefficient with an increase in concentration would speed up the concentration equalization. Therefore, the inclusion of concentration dependences of the diffusion coefficients leads to nothing more than an enhancement of the effect obtained in the computations.

We believe that the effect of diffusion on the distribution of dissolved substances will be similar in character with the inclusion of radial flow: the spatial protein distribution will be determined primarily by the radial fluid flow, while the salt distribution will be nearly uniform.

Reyes et al. [18] investigated the effect of concentration and ionic strength of the solution on the albumin diffusion coefficient. Experiments showed that the albumin diffusion coefficient remained nearly constant over a wide concentration range. At the same time, increasing the ionic strength of the solution resulted in a significant decrease in the diffusion coefficient. The authors attribute this decrease in diffusion coefficient to the conformation transitions of proteins and probably to the aggregation of molecules. We emphasize that

[7] In the medical literature it is conventional to distinguish the osmotic pressure produced by dissolved salts and the osmotic pressure produced by dissolved proteins. The latter is termed the *oncotic* pressure.

it is the latter effect that appears to be particularly significant in the case of dehydration self-organization of biological fluids.

5. Convective processes in the evaporation of a droplet

Deegan et al. [13] proposed a possible mechanism for the emergence of a radial flow directed to the droplet center. This flow was attributed to the occurrence of the Marangoni instability — that is, the instability arising from the coordinate dependence of the surface tension coefficient. The instability development criterion is the Marangoni number

$$\mathrm{Ma} = \frac{\Delta\sigma R}{\rho\nu\alpha}\,, \tag{9}$$

where σ is the surface tension coefficient, $\Delta\sigma$ is the change in the surface tension coefficient along the surface, ρ is the density, ν is the kinematic viscosity coefficient, α is the thermal diffusivity, and R is the droplet radius (the characteristic dimension over which there arises the change in the surface tension coefficient).

The development of the Marangoni instability is commonly associated with the temperature dependence of the surface tension coefficient. Since the temperature of the upper part of a droplet is higher than the temperature of the lower one, the surface tension coefficient varies from point to point (Fig. 6). However, for a biological fluid droplet it seems that the dependence of the magnitude of the surface tension coefficient on the concentration of dissolved substances may be an effect of greater significance.

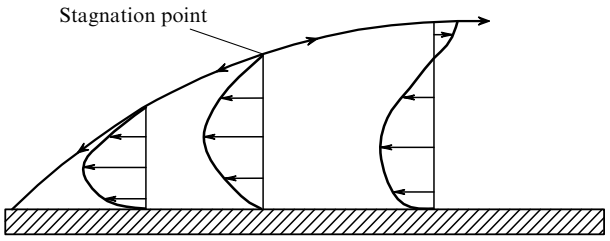

Figure 6. Emergence of a flow caused by the difference in surface tension coefficients.

6. Influence of a salt admixture on the character of cracking of a drying colloidal solution

Pauchard et al. [15] analyzed the influence of physicochemical properties on the crack pattern produced in the evaporation of a colloidal suspension droplet on a flat substrate. Different types of crack patterns were observed, depending on the salt content in the suspension: for low salt concentrations there form uniformly arranged radial cracks which go from the droplet edge to its center; for a medium salt content, the cracks are chaotically located, and for a high salt content there forms one circumferential crack. These properties are related to the variation of the droplet shape during evaporation, and the droplet shape in turn depends on the salt content in the suspension. For a medium salt content, strong perturbations of the droplet shape emerge, which can be interpreted as the kink instability.

Experiments were performed with the aqueous sol of silicon oxide. The particle radii were equal to 15 ± 2 nm. The droplet volume was 5 mm^3. (Notice that the sol particles are comparable to albumin globules in size; the fluid volume is three times smaller than that employed in medical practice and in Ref. [17].) For a substrate, use was made of a carefully cleansed microscope slide. The character of cracks was found to be related to the competition between gelation and droplet evaporation. A linkage was established between the characteristic times of these processes and the crack pattern.

In the absence of evaporation, the stability of aqueous colloidal suspensions is determined by the interaction of colloidal particles, i.e., the competition between the van der Waals attraction and electrostatic repulsion. With an increase in the salt content in the colloidal solution there occurs screening of the electrostatic interaction with the consequential gelation or flocculation, depending on the fractional volume occupied by the colloidal particles.

In the experiments conducted, the volume fraction of the particles was equal to 0.2; therefore, the addition of salt was invariably followed by gelation. The ionic strength I of a solution[8] was varied between 0.04 and 0.6 mol l^{-1}. The contact angle is independent of the ionic strength I: $\theta \approx 40^\circ$. According to the rheologic measurements conducted, the sol–gel transition in this case is adequately described by a conventional percolation model. The gelation time t_g was shown to depend heavily on the ionic strength of a solution: for $I \leqslant 0.2$ mol l^{-1}, t_g exceeds one day, while for $I \geqslant 0.4$ mol l^{-1} $t_g < 100$ s.

Therefore, by changing the ionic strength of a solution it is possible to vary the gelation time over wide limits. For quantitative characteristics, advantage can conveniently be taken of the characteristic evaporation time

$$t_d = \frac{R_0}{\omega}\,,$$

where R_0 is the radius of the droplet base, and $\omega = -S^{-1}\,\mathrm{d}V/\mathrm{d}t$ is the average flux of the water evaporating from a unit area of the droplet per unit time. Experiments showed that the latter quantity is independent of the time and the ionic strength as long as the condition $\Delta V/V \leqslant 30\%$ holds true.

When the solvent evaporates, the ion and sol particle concentrations increase, thereby resulting in a change in the gelation time at a given point. The authors of the work believe that the local ionic strength of a solution and the volume fraction of colloidal particles can never become lower than their initial values. Therefore, t_g constitutes the upper limit for suspension gelation time in the course of drying.

As noted in Section 3, the drying of a gel droplet proceeds with a constant contact area, unlike the drying of a pure fluid droplet, which proceeds with a constant contact angle. The nonuniform distribution of colloidal particles in the droplet and the difference in ionic strengths of solutions are responsible for a change in mechanical properties, which results in a deviation of the droplet shape from a spherical segment.

For a low ionic strength of a solution ($I \geqslant 0.18$ mol l^{-1}), the gelation time exceeds the evaporation time ($t_g/t_d > 100$). The particles and the ions accumulate near the interphase boundary; a gel layer builds up at the droplet edge, while the

[8] It is noteworthy that the ionic strength of blood serum is equal to about 0.15 mol l^{-1}.

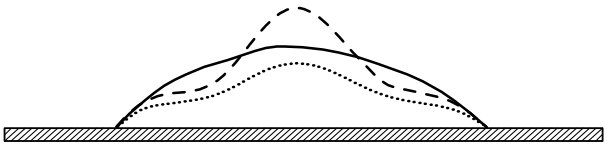

Figure 7. Schematic representation of the droplet profile dynamics on emergence of the buckling instability. The solid, dashed, and dotted lines depict the sequence of droplet profile variations.

central part of the droplet remains liquid. As the solvent evaporates, the central part of the droplet decreases. The gel ring at the droplet edge tends to contract and a strong mechanical stress emerges. The stress is primarily orthogonal, since the gel is firmly attached to the substrate. At the point in time t_c, the stress becomes strong enough to give rise to the first crack which originates in the interphase boundary line. During the next 60 s, a pattern of regularly arranged cracks forms at the droplet edge.

For an intermediate ionic strength $0.18 \leqslant I \leqslant 0.4$ mol l^{-1}, the gelation time and the evaporation time are the quantities on the same order of magnitude. The ratio t_g/t_d ranges from 0.1 to 10. The initial droplet evolution corresponds to the one described above: a gel ring forms initially at the droplet edge, while the central part remains liquid. At the point in time t_b, the droplet shape undergoes a change: the gel ring ceases to widen, and strong distortions in the central part of the droplet emerge. In particular, the height of the central part of the droplet ceases to decrease, then begins to increase, following which it decreases again (Fig. 7). The droplet surface in the central part is a gel film, while the interior part of the droplet remains liquid. The authors attribute the observed phenomenon to the buckling instability. The gel film on the droplet surface is rather porous and does not impede the solvent evaporation. As a result, the volume of the fluid confined under the surface becomes smaller, while the area of the film itself remains invariable.

The droplet shape distortion in the evaporation is typical not only for the albumin solution, but also for the solution of, for instance, dextran polysaccharide [19, 20]. In the latter case, a secondary instability additionally occurs, and the droplet acquires the shape of a honeycomb. The authors of Ref. [19] attribute the occurrence of the buckling instability to the fact that the shape of a 'Mexican hat' is energetically more advantageous than the shape of a spherical segment.

For intermediate values of the ionic strength, a chaotic crack pattern forms. The first crack originates at the droplet edge, passes through the center, stops slightly short of the opposite edge, and returns back to form a loop. About 60 s later, new cracks begin to initiate, thus forming a chaotic crack pattern.

For a high ionic strength ($I > 0.4$ mol l^{-1}), the gelation time is shorter than the evaporation time ($t_g/t_d < 10^{-2}$). The entire droplet rapidly passes into a gel. There emerge small distortions of the droplet shape (a weak buckling instability). The first crack originates near the interphase boundary and goes along the droplet edge to produce a circumferential crack. For a very high ionic strength, within several minutes secondary radial cracks additionally emerge.

Therefore, the formation of radial or chaotic crack patterns is typical for the drying droplet of a colloidal solution. The character of cracking is related not to the biological origin of the solution but is determined exclusively by the ratio between the gelation time of the solution and the rate of its evaporation.

7. Investigation of bovine albumin and sodium chloride solution

In a series of works by Annarelli et al. [5, 21, 22], Tarasevich and Ayupova [17], and Reyes et al. [18], an investigation was made of the aqueous solution of bovine serum albumin (BSA) and sodium chloride.

In Ref. [5], atomic-force microscopy techniques were employed to investigate the dendritic crystal growth in a thin gel layer of the BSA and sodium chloride solution. The crystals grow in the form of dendrites with perpendicular branches. The crystals typically measure several hundred micrometers. Secondary branches are observed along only one face and are equally spaced at about 30 micrometers. The secondary growth is controlled by way of formation of triangular crystallites along the opposite face and sealing of the edges. No apparent phase separation between BSA and NaCl was observed in the bulk, but the triangular crystallites are supposedly NaCl crystals, and therefore a local mesoscopic phase separation is observed. The last-mentioned statement is highly intriguing, for a preliminary spectroscopic investigation carried out in Ref. [6] revealed a close-to-unity correlation coefficient for the spatial distributions of Cl and S entering in the composition of proteins. On the other hand, the statement contradicts the main idea underlying the work [23].

In Ref. [21], contact and contactless scanning atomic-force microscopy was employed to investigate the influence of biologically and medically important salts of Na, K, Li, Mg, Ca, Ni, Co, Cr, Fe, and Cl on the ordinary and dendritic crystallization of an aqueous BSA solution. Four structural classes were observed, depending on the cationic nature:

(i) nonstructured aggregates of salt and albumin;
(ii) large mesocomposites of salt and protein;
(iii) mixed gels of salt and protein;
(iv) microscopic phase-layered systems.

In Ref. [22], an investigation was made of the crack pattern produced in the drying of a droplet of the BSA – NaCl solution with a volume of 15 mm^3 on a glass substrate. Use was made of solutions with different BSA concentrations and an ionic strength $I = 0.2$ mol l^{-1}. The solution is a gel, and the BSA molecules constitute ellipsoidal particles measuring $4 \times 4 \times 14$ nm^3. In all cases, the volume fraction of protein in the solution was equal to several percent. Given in Ref. [22] are the data for solutions with concentrations of 10, 20, 30, 40, and 60 g l^{-1}. It was noted that dendrites were produced in the central part of the dried-up droplet for the first three concentrations, and small chaotic cracks were observed in the latter cases.

Experiments were performed to confirm that albumin did not undergo chemical transformations in the course of drying. To determine the gelation time, recourse was made to measurements of the electrical conductivity of the droplet along its diameter. The current-vs-time curve demonstrates a jumpwise reduction of current by three orders of magnitude, corresponding to the point in time at which the gel phase propagates through the entire droplet volume. The portions of the curve relating to the sol and gel phases decline smoothly.

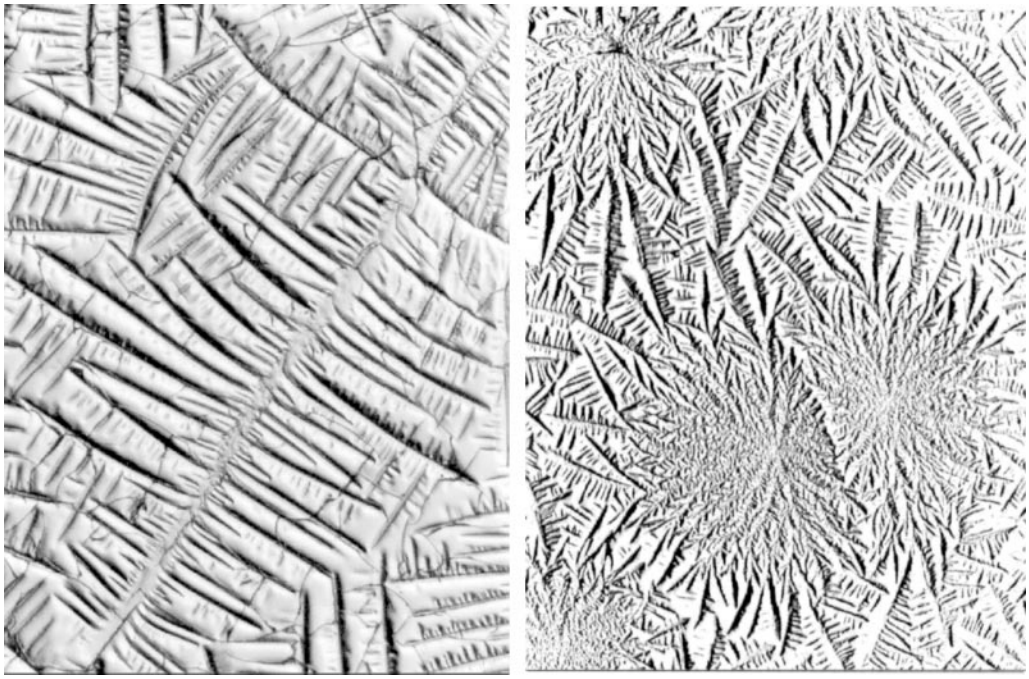

Figure 8. Dendrite in the samples of the aqueous solution of 0.9% NaCl and 8% albumin (at the left), and of 0.9% NaCl and 11% albumin (at the right). Both photographs were obtained at a similar magnification; the region measures about 1 mm.

Measurements were made of the dried-up droplet height employing the holographic interferometry, and the film thickness was shown to increase towards the edges.

The authors note that, unlike the case of inorganic sol [15], only regular radial cracks were observed; chaotic cracking was absent, although the experiments were conducted in cases where $t_c < t_g < t_d$. The authors attribute this to the fact that no gel crust emerged on the surface of the central liquid part of the droplet in their experiments, and no buckling instability was accordingly observed. It is pertinent to note that in the experiments use was made of solutions with a low protein content. As emphasized above, the droplet height-vs-time plot can be interpreted as the emergence of a weak buckling instability.

In addition, the dependence of the crack widths on the solution concentration and the distance to the droplet center was investigated by Pauchard et al. [15].

Aqueous BSA – NaCl solutions with a concentration of up to 120 g l^{-1} and an ionic strength of 0.15 mol l^{-1} were investigated in Ref. [17]. It was noted that the visual appearance of the central part of the droplet was significantly dependent on the BSA concentration (Fig. 8).

The effect of various external actions (heating, excess of salt) on the protein solution (BSA) was attributed by Reyes et al. [18] to the efficient dynamic process — diffusion. The method of holographic interferometry was employed to conduct measurements which hold interest for transfer studies. It was found that the diffusion coefficient is independent of the BSA concentration but depends significantly on the ionic strength of the solvent and on the heating, and that both effects are responsible for conformation transitions in albumin. This is evident from photon correlation spectroscopy (PCS) data. In all cases, the increase in protein size results in a decrease of the diffusion coefficient.

8. Formation of spiral structures

The emergence of spiral structures (Fig. 9) in the dehydration of human blood serum is considered to be an indication of pathology — hyperproteinemia (excessive content of proteins) [2]. Experiments with model fluids showed that spiral structures emerge only when the albumin concentration exceeds that in the blood plasma of a healthy person [17]. Golbraikh et al. [10] posed a model for describing the formation of such structures, which is based on the notion that mirror symmetry is absent in protein conglomerates that

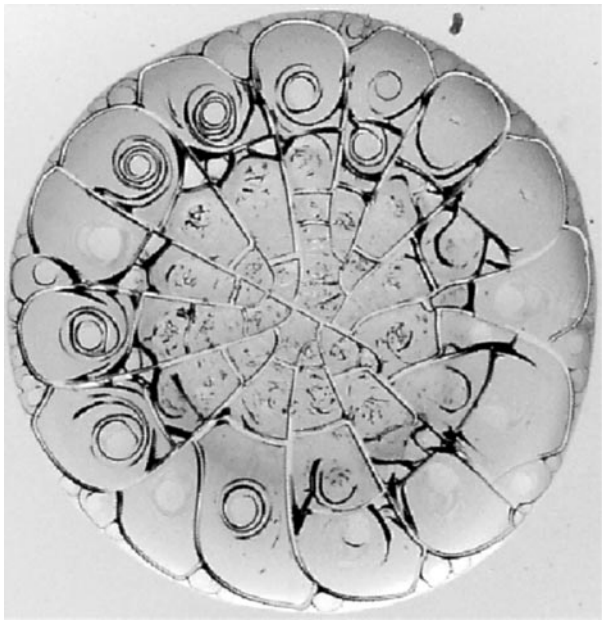

Figure 9. Spiral structures in a sample with 10% albumin and 0.9% NaCl.

make up liquid crystals. They proposed a criterion which relies on the ratio between the Frank parameters χ_2 and χ_3.

9. Production of crystalline structures

As noted above, it is possible to observe crystalline dendrites in the central part of a dried-up sample of blood serum and model liquids. Opinions differ widely concerning the nature of these crystals. In particular, in the view of Shabalin and Shatokhina [2] these dendrites are made up of salt crystals. Martyushev et al. [23 – 26] believe that phase layering of proteins and salt occurs. Annarelli et al. [5, 21] point to the absence of visible phase solution layering and suppose the crystals to be protein – salt mesocomposites; at the same time, the triangular crystals appeared along one of the dendrite faces are supposedly salt crystals. Spectroscopic investigation [6] does not give grounds to state that the crystals are made up of salt and are more likely to confirm that the separation into the salt and protein phases does not occur.

In connection with the contradictory character of the information, the elucidation of the chemical dendrite composition admittedly invites further experiments.

Due to the uncertainty in chemical dendrite composition, the works concerned with the modeling of salt crystal growth in the presence of proteins most likely have no direct relationship to the phenomena discussed in our review. It nevertheless seems appropriate to list some of the papers published in this area.

To date, efficient methods of dendrite growth modeling have been elaborated and are extensively used. These methods correctly include the anisotropy of surface energy, capillary effects, fluctuations, etc. (see, for instance, Ref. [27]). However, these simulations are conducted primarily for the crystal growth from a melt. The simulations are extremely arduous and call for large computer resources. In the available literature, we failed to find references to the application of this method to the modeling of dendrite crystal growth from a protein – salt solution.

Martyushev et al. [28] posed a τ-model — that is, a simple model for the description of dendrite crystal growth from a solution. In subsequent papers [23 – 26], the τ-model was further elaborated and employed to describe the dendrite growth of salt crystals in the presence of proteins. The modified model assumes that proteins are completely driven out by the growing crystal at the crystal – solution interface, with the effect that proteins are accumulated near the crystal surface.

Tarasevich [29, 30] performed an analysis which yielded the following.

(i) The τ-model [28] is an explicit computational scheme for the two-dimensional diffusion equation

$$\frac{\partial C}{\partial t} = D\left(\frac{\partial^2 C}{\partial x^2} + \frac{\partial^2 C}{\partial y^2}\right), \tag{10}$$

where C is the salt concentration in the solution, and D is the diffusion coefficient. The boundary conditions at the crystal – solution interface follow from the substance conservation law [31]

$$D\,\frac{\partial C}{\partial n} = \frac{(\rho - C)(C - C_0)}{\rho}\,\beta, \tag{11}$$

where $\partial C/\partial n$ is the derivative normal to the interphase boundary, ρ is the density of salt, β is the kinetic crystallization coefficient, and C_0 is the initial concentration of salt in the solution.

(ii) The τ-model contains no physical mechanisms (fluctuations, anisotropy of the surface energy, etc.) which could be responsible for the dendritic crystal growth.

(iii) Errors were committed in the realization of the model (too long a time step, an incorrect rule for concentration recalculation), which cast doubt on the reliability of the results obtained.

Tarasevich et al. [32] analyzed several mechanisms which might be responsible for the salt dendritic crystal growth.

Therefore, it is valid to say that at present there is no model furnishing an adequate description of the shape variation of dendrites that grow from a protein – salt solution.

10. Variation of the magnetic properties of a protein solution during drying

Rapis [11] described experiments with a protein solution (lysozyme). Iron filings were deposited on the surface of the sample, with copper and aluminum filings deposited on the surface of controls. The experimental samples and the controls were held under similar macroconditions. The investigation showed that the solidification of experimental samples was accompanied by a qualitative change of the observed structures. It was hypothesized that protein becomes magnetically sensitive on solidification. A hypothesis was proposed for the occurrence of magnetohydrodynamic instability in the condensation of proteins.

We were unable to find information on research in this area, and therefore the question of magnetic sensitivity of proteins is still an open one.

11. Structural changes upon electromagnetic action

In several papers [2, 9], the authors observed changes in the structures produced in the dehydration of biological fluids after they were subjected to physical action. Investigations were made of the effects of low-intensity blue and red light, a vortical magnetic field, millimeter (EHF) waves, He – Ne laser light, and temperature action (freezing – defrosting). It has been suggested [9] that the liquid crystal phase of the proteins changed under the physical actions.

We believe that additional experiments are called for, which could confirm or refute the hypothesis advanced.

12. Conclusions

The above analysis of the data available from the literature allows the drawing of the following generalized picture of the processes occurring in the dehydration self-organization of biological fluids.

(1) The evaporation of the droplet of a biological fluid from the substrate surface proceeds for an invariable contact surface owing to the pinning of the interphase boundary line.

(2) The evaporation is determined by the vapor diffusion in the air.

(3) There emerge in-droplet radial fluid flows directed towards the droplet edge. These flows transfer colloidal particles and dissolved substances to the periphery of the droplet.

(4) A radial flow directed towards the droplet center emerges in the surface layer of the droplet. The underlying

cause of this flow is the development of Marangoni instability.

(5) Gelation and cracking of the gel produced begin at the periphery of the droplet. The character of the crack pattern may be regular or chaotic, depending on the gelation–evaporation time ratio.

(6) For a specific gelation–evaporation time ratio, the droplet shape can experience strong distortions (the buckling instability) caused by the fact that the droplet surface has turned into a gel, while the central part remains a sol.

(7) Further dehydration leads to the production of nuclei (concretions). The chemical composition of these structures and the cause of their production remain unknown.

(8) Variously shaped crystal structures or small chaotic crack patterns may be formed in the central part of the sample. The resultant crystal shape is extremely sensitive to the initial protein concentration in the fluid.

(9) For high protein concentrations, the emergence of spiral structures is observed, whose origin can be explained on the basis of liquid crystal theory.

(10) Additional small structures (plaques, wrinkles, etc.) may be formed in the dehydration of biological fluids obtained from patients. Some of these structures bear similarities to those observed in drying a droplet of liquid with a low concentration of dispersed particles, which may count in favor of the common production mechanisms for these structures.

The above list of processes should by no means be considered as complete, comprising only those processes whose influence on the structure formation is more or less clear. Mention can be made of a number of processes that can exert an effect on structure formation during the dehydration of a biological fluid droplet, but determining the character of this effect calls for further investigation. To these processes may belong droplet oscillations related to the bending of the droplet shell [33, 34], as well as to the formation of different phases [35–37]. Furthermore, the mobility of different phases is influenced by the redistribution of dissolved air [38].

It is worth indicating the problems whose solution would be worthwhile both from the theoretical and practical standpoints.

(1) A more precise definition of the distribution of substances in the dried droplet of a biological fluid, in particular, determination of the chemical composition of nuclei (concretions), crystal structures, and structures typical for pathological processes (plaques, Sierpinski's carpets, Arnold's tongues).

(2) A more precise exposition of the effect of physical action (primarily, the effect of electromagnetic fields) on the physicochemical properties of biological fluids.

(3) Elucidation of the relationship between the processes occurring in an organism and the variation of the physicochemical properties of biological fluids, in particular, the variation of the ionic strength of biological fluids, gelation time, and viscosity.

(4) A more rigorous inclusion of the effect of diffusion on the distribution of the components of a biological fluid in the course of its dehydration.

(5) Taking into account the vertical distribution of substances in a droplet during dehydration.

(6) Construction of a correct model describing the formation of crystal structures in the dehydration of biological fluids.

(7) Construction of a dynamic gelation model with the inclusion of nonuniform substance distribution and the complex geometry of the object.

(8) Construction of a quantitative model focusing on the development of the buckling instability of the droplet of a biological fluid during dehydration.

(9) Inclusion of the effect of droplet oscillations.

(10) Inclusion of the influence of the air dissolved in the droplet on the mobility of different phases.

(11) Construction of the models describing the formation of small structures (plaques, wrinkles, Sierpinski's carpets, and Arnold's tongues).

To summarize, it is valid to formulate the following statement: the processes of dehydration self-organization of biological fluids are physical and physicochemical in nature and can be described in the context of conventional approaches. Undoubtedly, revealing the relationship between the pathological processes occurring in an organism, the variation of the physical and physicochemical properties of the biological fluids caused by these processes, and the form of the structures produced in the drying of the droplet of a biological fluid are of theoretical and practical interest.

References

1. Rapis E G, Gasanova G Yu *Zh. Tekh. Fiz.* **61** (4) 62 (1991) [*Sov. Phys. Tech. Phys.* **36** 406 (1991)]
2. Shabalin V N, Shatokhina S N *Morfologii Biologicheskikh Zhidkosteĭ Cheloveka* (Morphologies of Biological Human Fluids) (Moscow: Khrizostom, 2001)
3. Rapis E G *Zh. Tekh. Fiz.* **71** (10) 104 (2001) [*Tech. Phys.* **46** 1307 (2001)]
4. Shabalin V N, Shatokhina S N *Vestn. Ross. Akad. Med. Nauk* (3) 45 (2000)
5. Annarelli C et al. *Cryst. Eng.* **2** (1) 79 (1999)
6. Amantaeva L S, Thesis for Master's Degree in Physicomathematical Sciences (Astrakhan': Astrakhan' State University, 2003)
7. Lekhin I V et al. (Eds) *Slovar' Inostrannykh Slov* (Dictionary of Foreign Language Words) 13th ed. (Moscow: Russkiĭ Yazyk, 1986)
8. Rapis E G *Zh. Tekh. Fiz.* **72** (4) 139 (2002) [*Tech. Phys.* **47** 510 (2002)]
9. Yakhno T A et al. *Zh. Tekh. Fiz.* **73** (4) 23 (2003) [*Tech. Phys.* **48** 399 (2003)]
10. Golbraikh E, Rapis E G, Moiseev S S *Zh. Tekh. Fiz.* **73** (10) 116 (2003) [*Tech. Phys.* **48** 1333 (2003)]
11. Rapis E G *Pis'ma Zh. Tekh. Fiz.* **23** (7) 28 (1997) [*Tech. Phys. Lett.* **23** 263 (1997)]
12. Deegan R D et al. *Nature* **389** 827 (1997)
13. Deegan R D et al. *Phys. Rev. E* **62** 756 (2000)
14. Deegan R D *Phys. Rev. E* **61** 475 (2000)
15. Pauchard L, Parisse F, Allain C *Phys. Rev. E* **59** 3737 (1999)
16. Schroeder M *Fractals, Chaos, Power Laws: Minutes from an Infinite Paradise* (New York: W.H. Freeman, 1991) [Translated into Russian (Izhevsk: RKhD, 2001)]
17. Tarasevich Yu Yu, Ayupova A K *Zh. Tekh. Fiz.* **73** (5) 13 (2003) [*Tech. Phys.* **48** 535 (2003)]
18. Reyes L et al. *Colloids Surf. B: Biointerfaces* **25** (ER2) 99 (2002)
19. Pauchard L, Allain C *Europhys. Lett.* **62** 897 (2003)
20. Pauchard L, Allain C *C.R. Phys.* **4** 231 (2003)
21. Annarelli C et al. *Cryst. Eng.* **3** (ER3) 173 (2000)
22. Annarelli C et al. *Eur. Phys. J. E* **5** 599 (2001)
23. Martiouchev L M, Seleznev V D, Skopinov S A *J. Stat. Phys.* **90** 1413 (1998)
24. Martyushev L M, Seleznev V D, Skopinov S A *Pis'ma Zh. Tekh. Fiz.* **22** (16) 12 (1996) [*Tech. Phys. Lett.* **22** 648 (1996)]
25. Martyushev L M, Seleznev V D, Skopinov S A *Pis'ma Zh. Tekh. Fiz.* **23** (13) 1 (1997) [*Tech. Phys. Lett.* **23** 495 (1997)]

26. Martyushev L M, Seleznev V D *Pis'ma Zh. Tekh. Fiz.* **25** (20) 71 (1999) [*Tech. Phys. Lett.* **25** 833 (1999)]
27. Warren J A, Boettinger W J *Acta Metall.* **43** 689 (1995)
28. Martyushev L M, Seleznev V D, Skopinov S A *Pis'ma Zh. Tekh. Fiz.* **22** (4) 28 (1996) [*Tech. Phys. Lett.* **22** 146 (1996)]
29. Tarasevich Yu Yu *Zh. Tekh. Fiz.* **71** (5) 123 (2001) [*Tech. Phys.* **46** 627 (2001)]
30. Tarasevich Yu Yu *Mat. Modelirovanie* **13** (8) 117 (2001)
31. Vaĭnshteĭn B K (Ed.-in-Chief) *Sovremennaya Kristallografiya* (Modern Crystallography) Vol. 3. Chernov A A et al. *Obrazovanie Kristallov* (Crystal Growth) (Moscow: Nauka, 1980) [Translated into English (Berlin: Springer-Verlag, 1986)]
32. Tarasevich Yu Yu, Konstantinov V O, Ayupova A K *Izv. Vyssh. Uchebn. Zaved. Severo-Kavkazskiĭ Region Estestv. Nauki* (Special Issue. Mathematical Modeling) 147 (2001)
33. Lewis J B, Pratt H R C *Nature* **4365** 1155 (1953)
34. Kostarev K G, Briskman V A *Dokl. Ross. Akad. Nauk* **378** 187 (2001) [*Dokl. Phys.* **46** 349 (2001)]
35. Stoĭlov Yu Yu *Usp. Fiz. Nauk* **170** 41 (2000) [*Phys. Usp.* **43** 39 (2000)]
36. Ivanitskiĭ G R et al. *Dokl. Ross. Akad. Nauk* **374** 548 (2000) [*Dokl. Biophys.* **373**/375 41 (2000)]
37. Ivanitskiĭ G R et al. *Dokl. Ross. Akad. Nauk* **375** 685 (2000) [*Dokl. Biophys.* **373**/375 56 (2000)]
38. Ivanitsky G R, Kravchenko V V, Tsyganov M A *Dokl. Ross. Akad. Nauk* **383** 263 (2002) [*Dokl. Biochem. Biophys.* **383** 88 (2002)]
39. Rapis E G *Zh. Tekh. Fiz.* **70** (1) 122 (2000) [*Tech. Phys.* **45** 121 (2000)]
40. Rapis E G *Pis'ma Zh. Tekh. Fiz.* **21** (10) 13 (1995) [*Tech. Phys. Lett.* **21** 321 (1995)]